JOURNAL OF SPACECRAFT AND ROCKETS
Vol. 32, No. 3, May–June 1995

Thermal Protection System Design Studies for Lunar Crew Module

S. D. Williams*
Lockheed Engineering and Sciences Company, Inc., Houston, Texas 77258-8561
Donald M. Curry†
NASA Johnson Space Flight Center, Houston, Texas 77058
and
Stanley A. Bouslog‡ and William C. Rochelle§
Lockheed Engineering and Sciences Company, Inc., Houston, Texas 77258-8561

This paper present the results of a trade study to predict aeroheating and thermal protection system (TPS) requirements for manned entry vehicles returning to Earth from the moon. The objectives of the study were to assess the effects of vehicle size and lunar return strategies on both the aerothermodynamic environment and the TPS design. The study guidelines were based on an Apollo Command Module (CM) configuration for scales of 1.0, 1.5, and 2.5. Lunar return strategies included direct entry and aerocapture followed by low Earth orbit entry. Convective heating was obtained by the boundary-layer integral matrix procedure code, and radiative heating was computed with the QRAD program. The AESOP-STAB code was used for TPS analysis for ablating materials, and the AESOP-THERM code was used for nonablating materials. Principal results indicated that there was an optimum size for minimum heating with the Apollo CM-shaped vehicles, although heating rates were not a strong function of vehicle size. Direct entry had significantly higher heating rates than aerocapture; however, aerocapture resulted in higher heat loads and TPS weight. The TPS weight factor (ratio of TPS weight to total vehicle weight) was 6–8% for all lunar return strategies using an Avco ablator on the forebody and FRCI-12/LI-900 on the aftbody, with the TPS weight being about 50% less than that of the original Apollo CM vehicle.

Nomenclature

C_D	= drag coefficient
C_L	= lift coefficient
L/D	= lift-to-drag ratio
S/R	= ratio of the wetted length measured from the vehicle centerline axis to the radius from the centerline to the torus
W/C_DA	= ballistic coefficient
α	= angle of attack
γ	= flight-path angle
η_T	= TPS weight fraction, expressed as a percentage of total vehicle weight

Introduction

A LONG-RANGE goal established by the Presidential Directive on National Space Policy of 1988 is "to expand human presence and activity beyond Earth orbit into the solar system." This directive has caused increased interest in the exploration of the solar system, which has been reflected in renewed awareness of activities related to the Space Exploration-Initiative (SEI). The First Lunar Outpost (FLO), which is part of the SEI master plan, is a series of missions to return man's presence to the lunar surface. Preliminary plans call for the first launch to be an unmanned cargo mission that places a habitat module on the lunar surface. The second launch would be manned by a crew of four, and the crew would land near the habitat, remain on the lunar surface for 45 days, and then return to Earth. Personnel at NASA Johnson Space Center have been conducting trade studies to provide the basis for decisions on the lunar return mission and vehicle design to meet a first launch date of 1999. In order to assist the system designers in these trade studies, crew-module concept design studies are being conducted. The crew module houses the crew during launch from Earth, during transit to and landing on the moon, and during lunar ascent and Earth return. Minimization of the crew-module weight is highly desirable, and program cost and schedule constraints suggest that simple and proven designs should be used. The initial crew-module design in a modified Apollo CM using currently flight-certified materials.

The TPS design requirements for manned spacecraft that enter Earth's atmosphere from a lunar orbit are more demanding than those required for the Space Shuttle Orbiter. This is due, in part, to the increased velocities required from vehicles entering from a lunar orbit instead of from LEO. Convective and radiative environments of vehicles entering the Earth's atmosphere from the moon were investigated 20 years ago. Lee and Goodrich,[1] for instance, compared pressure and convective-heating-rate history data on the Apollo CM with wind-tunnel data. Ried and Rochelle developed the QRAD program[2] to make Apollo CM radiative-heating predictions, which compared very well with Apollo 4 flight radiometer measurements.[3]

Three basic techniques can be used to return a vehicle from the moon to Earth: direct entry, aerocapture followed by direct entry after one orbit, and aerocapture followed by direct entry after several orbits. Thus, the objectives of this investigation are to assess the effects of the vehicle size and lunar return strategies on the aerothermodynamic environment and TPS weight, and to determine the weight factor using a common TPS design for all lunar return strategies. Three crew modules were selected to be evaluated with

Presented as Paper 93-2843 at the AIAA 28th Thermophysics Conference, Orlando, FL, July 6–9, 1993; received July 28, 1993; revision received Dec. 14, 1993; accepted for publication Jan. 3, 1994.

*Senior Engineer, Software Systems and Thermal Test Department, P.O. Box 58561, Mail Stop B14. Member AIAA.

†LESS Subsystem Manager, Thermal Branch, Structures and Mechanics Division, Mail Stop ES3. Member AIAA.

‡Principal Engineer, Navigation, Control, and Aeronautics Department, P.O. Box 58561, Mail Stop C87. Member AIAA.

§Senior Advanced Systems Specialist, Navigation, Control, and Aeronautics Department, P.O. Box 58561, Mail Stop C87. Associate Fellow AIAA.

Table 1 Vehicle mass and ballistic coefficients

Scale	Mass, kg	W/C_DA, kg/m^2	Ref. area, m^2	R, m	R_1, m
1.0[a]	5,668	379	11.6	1.96	4.69
1.0	6,466	432	11.6	1.96	4.69
1.5	11,724	348	26.0	2.94	7.04
2.5	34,198	366	72.4	4.90	11.73

[a]Original Apollo.

Table 2 Trajectory and aerodynamic parameters

Mode of entry	Initial velocity, km/s	γ, deg
Direct entry	11.0	−6.6
Aerocapture	11.0	−5.2
LEO entry	7.0	−1.5
Apollo 4	11.2	−6.95

Aerodynamic criteria
$\alpha = 20$ deg
$C_D = 1.2906$
$C_L = 0.3867$
$L/D = 0.3$

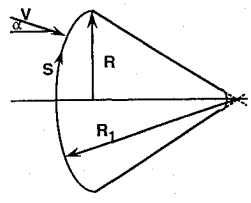

Fig. 1 Sketch of the lunar crew vehicle.

geometric scale factors of 1.0, 1.5, and 2.5 times the original Apollo CM (Fig. 1).

This paper discusses the crew-vehicle configurations, trajectory definitions, and aerodynamic heating. The TPS design and structural materials used in the analysis associated with the vehicle configurations for three missions—direct entry, aerocapture–1-orbit entry, and aerocapture–5-orbit entry—are presented. Results are presented which substantiate a common TPS design for both direct entry and aerocapture lunar return scenarios. The TPS designs using currently available flight-certified materials along with the trajectories selected provide a database for comparison with designs using advanced TPS materials.

Vehicle and Entry-Trajectory Design

Preliminary studies have been conducted in which 1.0-, 1.5-, and 2.5-scale Apollo vehicles were considered for both direct-entry and aerocapture–LEO-entry return strategies. Different vehicle configurations have been analyzed in previous studies.[4] This study specifically uses the Apollo shape to assess entry and geometrical parameters. Vehicle and trajectory parameters are shown in Tables 1 and 2.

The direct-entry cases used a slightly modified Apollo guidance scheme with no attempt to tune the guidance. The aerocapture cases used the Aeroassist Flight Experiment (AFE) guidance scheme, which required extensive tuning to achieve good targeting performance. The LEO cases used a derivative of the Shuttle Orbiter guidance with no tuning required.

The entry flight-path angles are determined by first establishing an entry corridor for the vehicle. The top of the corridor is the shallowest flight-path angle the vehicle can enter at and not skip while flying full lift down. The bottom of the corridor is the steepest the vehicle can enter and not exceed either the g limit or the heating limit while flying full lift up. It is desirable to fly near the middle of the corridor in order to be covered in case of dispersions in atmosphere, vehicle aerodynamics, etc. Generally, for direct entry, the vehicle is flown toward the steep side of the corridor to ensure capture, while for aerocapture, the vehicle is flown toward the shallow side to avoid capture. Thus, the entry-corridor width is a function of velocity and W/C_DA. While the design trajectories were affected by W/C_DA, the 20% variation in W/C_DA was not enough to change the corridor width, significantly and the corridors for the three sizes of vehicles are essentially the same.

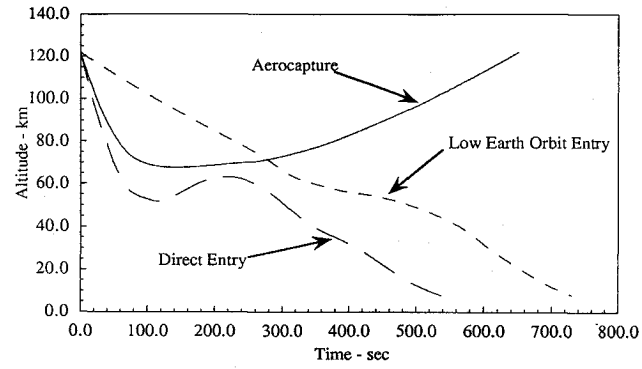

Fig. 2 Altitude as a function of time for the 1.5-scale Apollo CM for aerocapture, direct entry, and LEO entry.

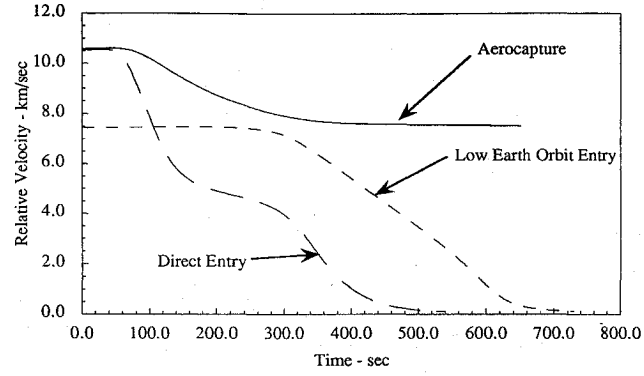

Fig. 3 Velocity as a function of time for the 1.5-scale Apollo CM for aerocapture, direct entry, and LEO entry.

Figures 2 and 3 present a comparison of the altitude and relative velocities for the 1.5-scale Apollo for the three types of trajectories considered. The aerocapture trajectory has a perigee of about 68 km, and the lowest point for direct entry before the altitude increases is about 53 km. The velocity for direct entry drops significantly during the first 50–200 s, in contrast with the aerocapture and LEO entries.

Crew Module Aerothermal Design Methodology

The reference cold-wall convective heating rates were obtained by using the BLIMP computer program[5] to compute the stagnation-point heating for an Apollo vehicle at 0-deg angle of attack. Pressure distributions near the stagnation point, which were obtained from wind-tunnel test data,[6] were input into BLIMP to determine the stagnation-point velocity gradient. The reference heating rates were multiplied by convective heating-rate distribution factors[7] (Fig. 4) to obtain the pitch-plane heating distribution for the vehicle at an angle of attack of 20 deg.

These heating distributions are shown as a function of S/R. Turbulence for Apollo occurred late in time and would not affect the TPS sizing. The distribution shown in Fig. 4 is valid for a real gas and has been substantiated from analysis of Apollo entry thermal performance. The Apollo wind-tunnel and flight pressure distributions were essentially the same.

The reference radiative heating rates were obtained by using the QRAD code[2] to compute the stagnation-point radiative heating to a sphere. The QRAD code uses a four-band model to compute the equilibrium radiation and a semiempirical correlation to compute the nonequilibrium radiation. This nonequilibrium radiation is based on binary scaling corrected by a collision limiting relation at high altitudes. Nonadiabatic and three-dimensional geometry effects are allowed for in both modes of radiation.

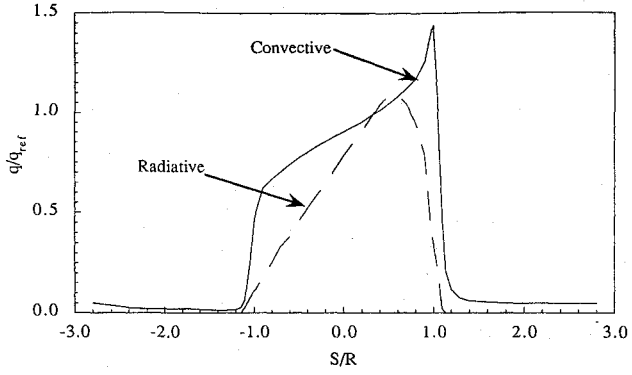

Fig. 4 Heating distribution factors for Apollo CM at $\alpha = 20$ deg.

Corresponding to the three different-sized vehicles—1.0, 1.5, and 2.5 scale—the sphere radii were 3, 4.6, and 7.6 m, respectively. Pitch-plane distributions of the radiative heating were obtained by multiplying the reference heating rate by radiative heating distribution factors derived analytically[3] (see Fig. 4).

Thermal Protection Design

Thermal protection systems were designed for these vehicle configurations using both flight-certified and advanced materials. The TPS design analysis is concerned with the short period of dominant heating during the pass through or into the atmosphere and subsequent thermal soakback. Reusable surface insulation (RSI) material selection was based on surface temperatures; an ablator was used where a RSI material could not be used.

Four flight-certified insulation materials were considered for this analysis[8]: AVCO-5026-H/CG, FRCI-12, (fibrous refractory composite insulation), LI-900 (Lockheed-insulation), and AFRSI (advanced flexible reusable insulation); see Table 3. AVCO-5026-H/CG is a charring ablator that was used for thermal protection on the Apollo CM. It consists of phenolic microballons embedded in a Novolac resin that is formed in phenolic honeycomb cells. This material has been previously flown at the flight entry conditions similar to those of the scaled crew-module vehicles.

The three flight-certified RSI materials were FRCI-12, LI-900, and AFRSI. For temperatures between 1483 and 1371°C, FRCI-12 is used. LI-900 would be used for temperatures below 1371°C and is coated with RCG in a manner similar to FRCI-12. Alternatively, AFRSI could be used for all temperatures below 983°C. Minimum thicknesses of 0.813 and 0.635 cm were used for all rigid tiles and blankets, respectively. Both FRCI-12 and LI-900 are bonded to NOMEX felt, which is bonded to the structure, whereas AFRSI is bonded directly to the structure. The felt acts as a strain isolation pad (SIP) between insulator and structure. RTV-560 is the bonding adhesive and has a temperature service limit of 288°C, whereas NOMEX felt has a temperature service limit of 444°C. The assumed thicknesses for the RTV-560 and felt are 0.1905 and 4.064 mm, respectively. RTV-560 is used to attach the ablator and the blankets to the structure. The material selected for the structure used in the thermal analysis consists of a lightweight honeycomb composite of graphite epoxy face sheets with a NOMEX paper honeycomb core (G/E Honeycomb). The structure design parameters are two 0.4064-mm graphite epoxy face sheets sandwiching the 3.81-cm honeycomb core with a maximum temperature service limit of 177°C.

Using certified materials for TPS design provides a database for performance comparison with developing or advanced TPS materials. Ceramic reusable surface insulation materials (rigid tiles and flexible blankets) being developed at the NASA Ames Research Center[9] and Lockheed Missiles and Space Company[10] were chosen for this comparison because of their expected higher reuse temperature (see Table 3). The rigid tiles assessed are the Ames alumina-enhanced thermal barrier (AETB) and the Lockheed high-thermal-performance (HTP) tiles. The flexible blankets considered are the Ames tailorable advanced blanket insulation (TABI) and the composite flexible blanket insulation (CFBI).

Analysis Methodology

The AESOP-STAB thermal analysis program[11] was used to calculate the minimum-weight TPS for the ablative system, and the AESOP-THERM thermal analysis program[12] was used to calculate the minimum weight TPS for RSI materials. Typically, the minimum-weight condition is subject to temperature constraints imposed on the backwall of selected materials. These programs are actually segregated into two parts: the optimization portion, which controls the numerical process to minimize the TPS, subject to the temperature constraints; and the thermal analysis portion, which calculates the thermal response of the system, subject to the initial and boundary conditions. Since only one material was permitted to vary in this analysis, a simple quadratic fit was selected for material minimization.

In summary, each TPS was optimized so that the structure never exceeded 177°C during the trajectory, subject to the minimum material condition. This calculation was performed with the appropriate program, AESOP-STAB or AESOP-THERM, with the heating factors discussed earlier. This produced selected values of TPS thickness and weight at the prespecified heating factors, which allowed the vehicle weight to be calculated.

The TPS weight fraction, expressed as a percentage of the total vehicle weight, used in this analysis is defined as

$$\eta_T = \frac{100 \times \text{TPS weight}}{\text{total vehicle weight}}$$

For vehicle designs requiring a TPS, the greatest benefits are derived for the system with the smallest value of η_T.

Results

Heating Rates and Loads

Comparison of the total, radiative, and convective heating-rate histories for a 1.5-scale Apollo vehicle at $S/R = 0.53$, the location of maximum total heating, for a direct-entry and an aerocapture trajectory are shown in Figs. 5 and 6, respectively. The direct-entry trajectory produces significantly higher heating peaks, but the aerocapture heat pulses are longer. Figure 7 presents a comparison

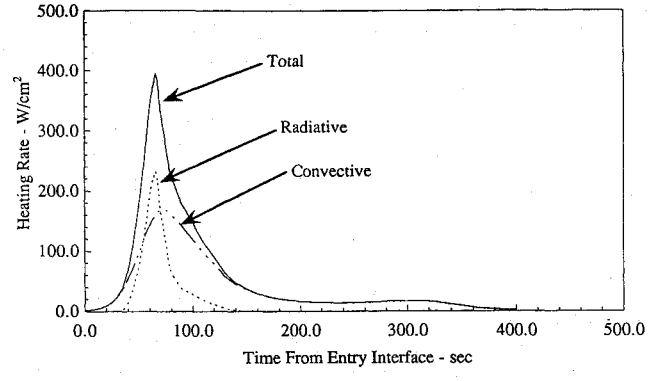

Fig. 5 Heating rates to a 1.5-scale Apollo vehicle at $S/R = 0.53$ for a direct-entry trajectory.

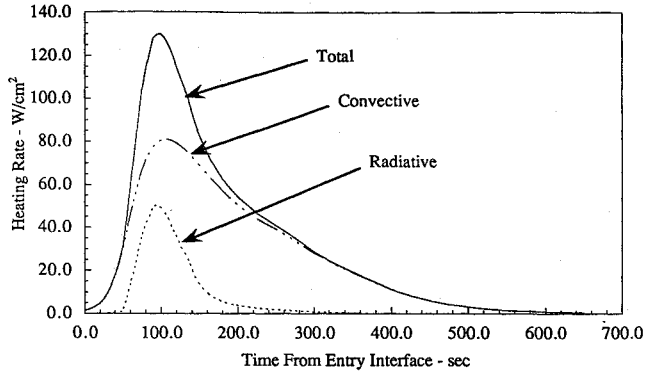

Fig. 6 Heating rates to a 1.5-scale Apollo vehicle at $S/R = 0.53$ for an aerocapture trajectory.

Table 3 Material characteristics

Materials	State[a]	Status[b]	Density, kg/m^3	Max. use temp., °C	Description
	v	f	513		
Avco-5026-H/CG	c	f	320		Charring ablator
RCG		f	1666	1538	Coating
FRCI-12		f	192	1483	RSI
LI-900		f	144	1371	RSI
AETB-8		a	128	1483	RSI
NOMEX		f	87	444	Felt
RTV-560		f	1410	288	Adhesive
AFRSI		f	149	983	Blanket
CFBI		a	149	1538	Blanket
TABI		a	160	1538	Blanket
GE Honeycomb		f	68	177	Composite structure

[a]v, virgin; c, char.
[b]a, advanced material—under development; f, flight-certified.

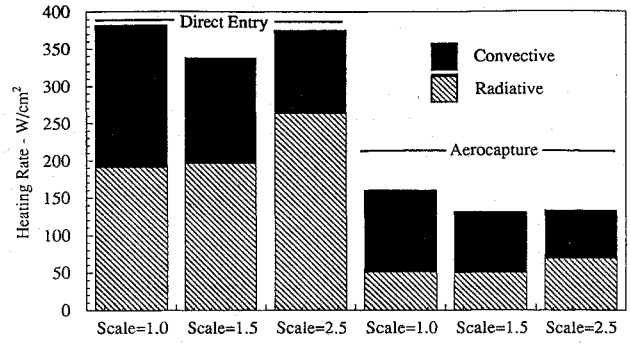

Fig. 7 Peak heating rates to Apollo-shaped vehicles by scale factor.

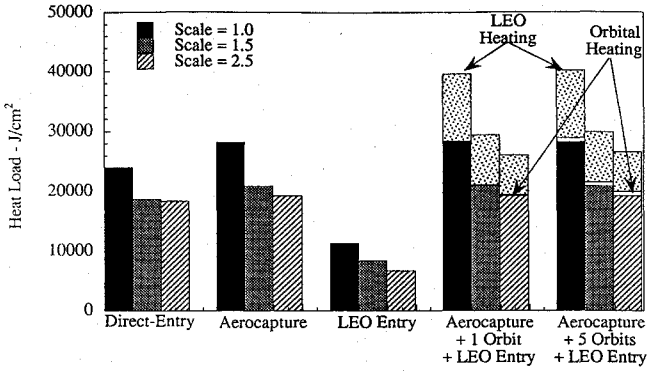

Fig. 8 Heat loads for Apollo-shaped vehicles at peak heating locations by scale factor.

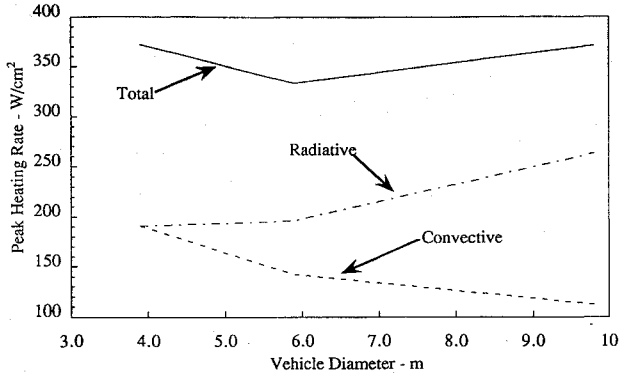

Fig. 9 Peak heating rates vs vehicle diameter for the direct-entry trajectory.

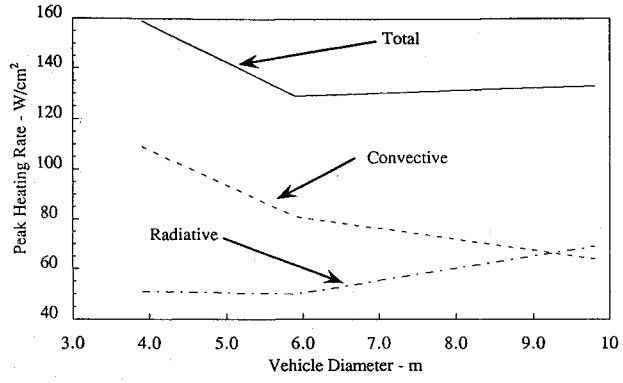

Fig. 10 Peak heating rates vs vehicle diameter for the aerocapture trajectory.

of the peak total heating rates at $S/R = 0.53$ for the three vehicles during direct-entry and aerocapture trajectories. The radiative heating is significantly decreased for the aerocapture trajectories, which results in significantly lower total heating rates. However, the heat pulse is longer for the aerocapture trajectories, and the heat loads are higher, as shown in Fig. 8. The combined heat load for the aerocapture–LEO-entry return strategy is significantly higher than that for the direct-entry case. However, a time span corresponding to one or several Earth orbits would separate the aerocapture and LEO entry heat pulses. This is illustrated in Fig. 8, where the on-orbit heating for one orbit and five orbits is presented for the aerocapture–LEO-entry analysis. This is somewhat misleading in that the longer orbital stay time actually reduces the TPS weight, since the initial TPS and structural temperatures are lower prior to entry. Table 4 presents a summary of the peak heating rates and heat loads for the different trajectories and different-sized vehicles.

The vehicle size also has an effect on the heating rates and loads. Figures 9 and 10 illustrate the variation of peak heating with vehicle diameter for both direct-entry and aerocapture cases. For the direct-entry trajectories, the 1.5-scale vehicle has a minimum total peak heating due to the decrease in convective heating, and only a small increase in radiative heating. At a scale of 2.5, the radiative heating increases significantly and more than compensates for the decreasing convective heating. The trends are similar for the aerocapture trajectories, but the radiative heating increases more slowly with increasing size. Hence, the result is that the 1.5- and 2.5-scale vehicles have similar peak total heating rates, as seen in Fig. 8. Heat loads for the larger vehicles are similar for the two entry cases, and they are significantly lower than the heat loads for the 1.0-scale vehicle.

Thermal Analysis Results

The thermal analysis results for both flight-certified and advanced materials are summarized in Figs. 11 and 12, which show the TPS unit weight versus heat load. The results shown for the 1.5-scale vehicle and the direct-entry trajectory are representative of the materials and the trajectories analyzed. Figure 12 illustrates that

Table 4 Summary of peak heating rates and heat loads for $S/R = 0.53$

Vehicle scale	Convective heating		Radiative heating		Total heating	
	Peak rate, W/cm^2	Heat load, J/cm^2	Peak rate, W/cm^2	Heat load, J/cm^2	Peak rate, W/cm^2	Heat load, J/cm^2
			Direct entry			
1.0	191	18,459	191	5,524	372	23,983
1.5	142	13,304	196	5,353	332	18,658
2.5	112	10,632	263	7,675	371	18,306
			Aerocapture			
1.0	109	24,272	51	3,956	159	28,228
1.5	81	17,045	50	3,774	129	20,818
2.5	64	13,891	69	5,319	132	19,209
			Low-Earth-orbit entry			
1.0	53	10,972	2.3	249	56	11,220
1.5	36	8,145	1.8	208	39	8,353
2.5	30	6,448	2.0	222	32	6,671

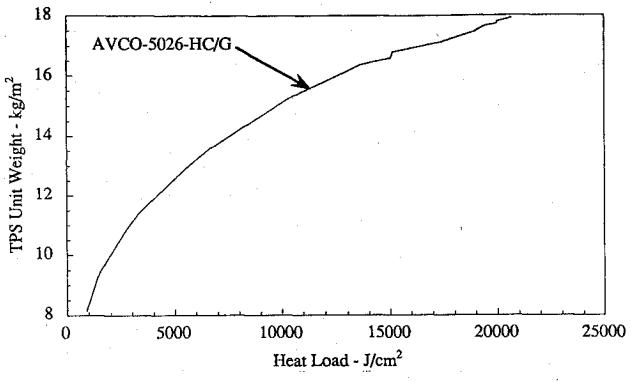

Fig. 11 Avco-5026 TPS unit weight vs heat load for the 1.5-scale Apollo CM for direct entry.

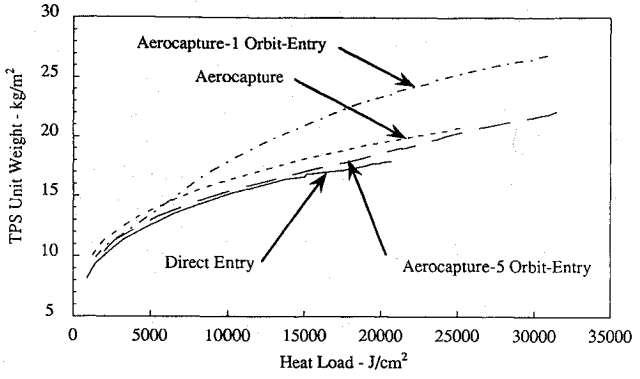

Fig. 13 Comparison of the Avco-5026 TPS unit weights vs heat load for the 1.5-scale Apollo CM.

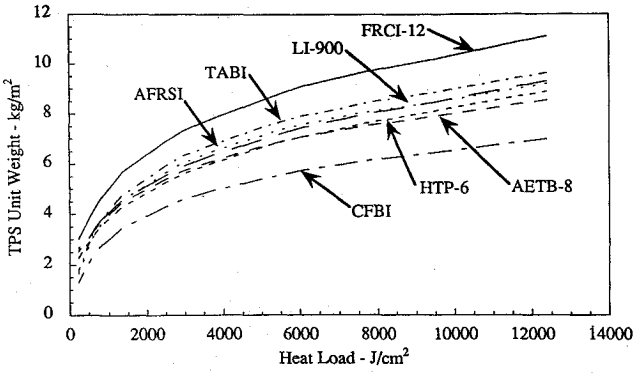

Fig. 12 Comparison of the TPS unit weights vs heat load for the 1.5-scale Apollo CM for direct entry.

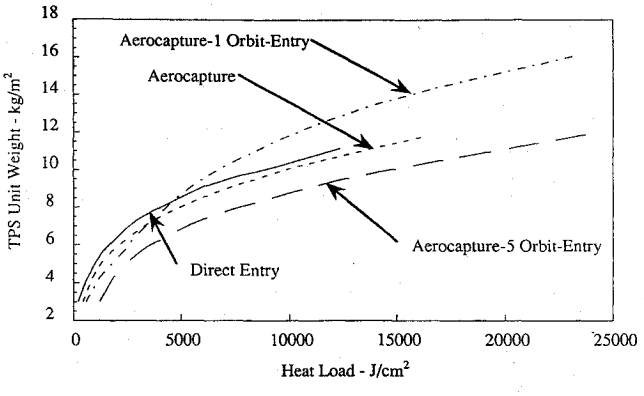

Fig. 14 Comparison of the FRCI-12 TPS unit weights vs heat load for the 1.5-scale Apollo CM.

the advanced blanket material, CFBI, can provide approximately 1-kg/m^2 weight reduction compared to the other reusable materials. The LI-900, AETB-8, and HTP-6 RSI materials have about the same TPS unit weights and are approximately 2 kg/m^2 lighter than FRCI-12.

The comparison between the different entry scenarios using the same material is shown in Figs. 13 and 14 for AVCO-5026 and FRCI-12, respectively. These support the concept that the preconditioning afforded by a longer orbital stay time can provide a measure of TPS efficiency. The extended soakback during orbit reduces the TPS temperature profile prior to entry.

Figures 11 and 13 present TPS unit weight comparisons for the vehicle's forebody, and Figs. 12 and 14 provide comparisons for the aftbody. Material selection is based on expected surface temperatures, as can be seen in Fig. 15. In Fig. 15 the three temperature

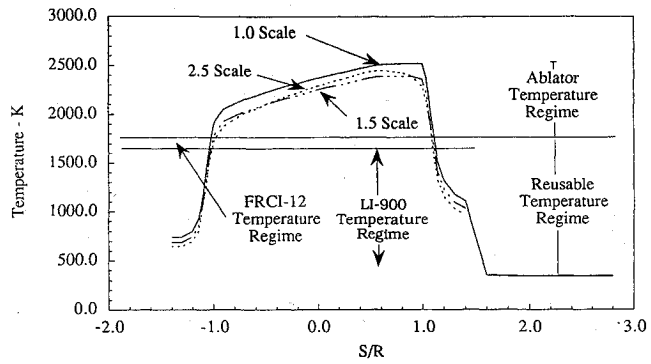

Fig. 15 Total temperature distribution on an Apollo vehicle for the time of peak heating during aerocapture.

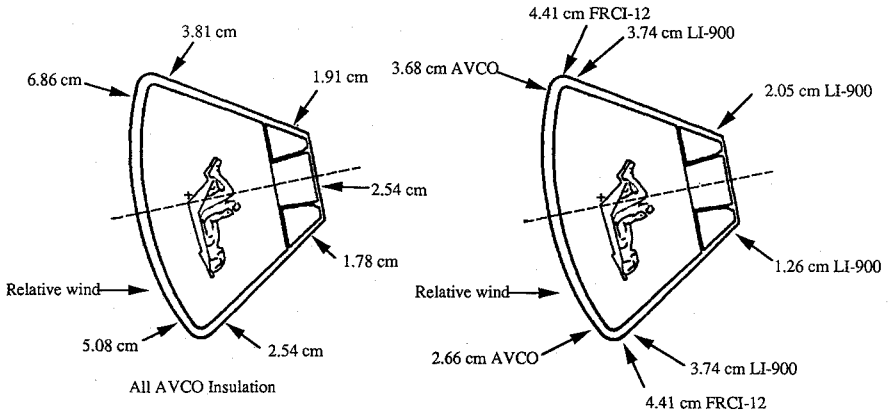

Material	Area (m^2)
AVCO	14.08
FRCI-12	0.33
LI-900	22.49

Fig. 16 Sketch of the insulation thickness for the original Apollo command module and 1.0-scale lunar crew module.

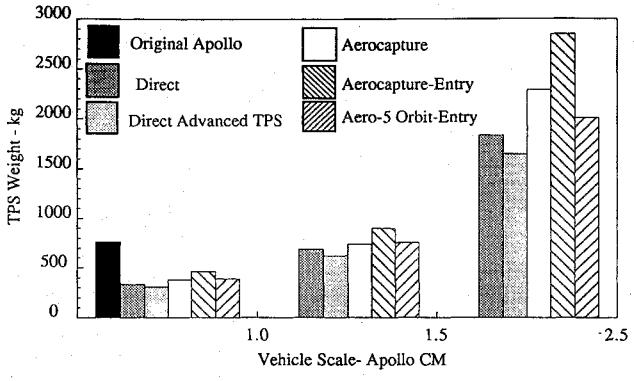

Fig. 17 TPS weight as a function of vehicle size.

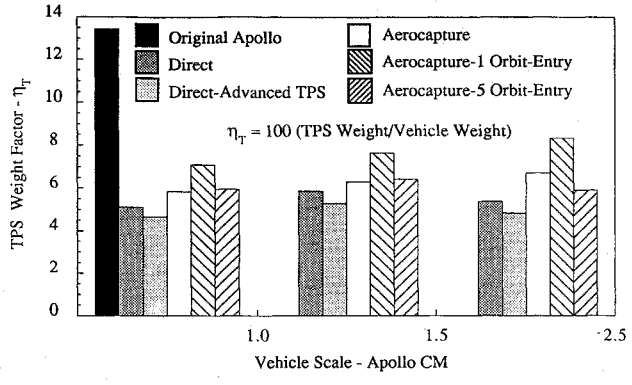

Fig. 18 TPS weight factor as a function of vehicle size.

regimes for the Avco ablator and FRCI-12 and LI-900 insulators are plotted as a function of S/R. This information is represented differently in Fig. 16, where the insulation thickness at selected points on the vehicle profile is shown. On this figure the thickness of the reusable insulation includes the insulation, SIP, and adhesive. Also shown in Fig. 16 is the comparative thickness of the ablator on the original Apollo CM.[13]

The original Apollo TPS was designed using two separate and distinct entry trajectories. A high-heating-rate entry trajectory was used to calculate the expected surface recession. A second trajectory, representing a high heat load, was used to calculate the TPS insulation thickness. Neither of these trajectories could be actually flown, but they were used as design conditions. The combination of these trajectories resulted in a TPS thickness that was conservative by a factor of two.

A comparison of the TPS weights as a function of vehicle size can be seen in Fig. 17. In this figure the TPS for the crew vehicles consists of AVCO-5026 HC/G, FRCI-12, and LI-900 except for the advanced TPS, which consists of AVCO-5026 HC/G and CFBI. The use of CFBI provides a 10% weight reduction in comparison with the FRCI/LI-900 insulation system. Figure 17 indicates that a 1.5-scale Apollo vehicle can be designed with a TPS weight equivalent to the original Apollo TPS weight using current technology. Flight experience showed that the surface recession was significantly less than predicted using the Arc-Jet test data and the high-heating-rate trajectory. Thus, by using current reusable materials (FRCI-12/LI-900) on the aftbody and sizing the ablator on the forebody to the anticipated entry heating, the TPS weight for a 1.0-scale vehicle can be reduced by 50% from the original design, as seen in Fig. 17.

A comparison of the TPS weight factors as a function of vehicle size can be seen in Fig. 18. This figure shows that the TPS weight factors for the aerocapture and aerocapture–5-orbit entry trajectories are essentially the same. In addition, η_T appears to be independent of vehicle size. Thus, for a small fractional increase in TPS weight, a common TPS design can be used to satisfy mission requirements independently of vehicle size and afford the opportunity to select a landing site at will. Figure 18 also shows that the calculated η_T for the original Apollo CM is double the calculated η_T for the crew vehicles analyzed in this study.

In this analysis the aerocapture entry trajectories were not rerun to take account of the additional propulsion requirements required for the subsequent entry, which would result in a 6% increase in entry weight. This additional increase weight was also not used in calculating the TPS weight factor.

Concluding Remarks

1) The effects of size of the lunar crew vehicles returning from the lunar outpost on the heating rates, TPS weight, and TPS weight factor were assessed for three Apollo CM-shaped vehicles with geometric scale factors of 1.0, 1.5, and 2.5 times the original CM.

2) Although there appears to be an optimum vehicle size for minimum heating, it was demonstrated that the peak heating rates are not a strong function of vehicle size. However, larger vehicles do have relatively lower heat loads.

3) The lunar retxurn direct entry has significantly higher heating rates, but the lunar return aerocapture has higher heat loads.

4) The TPS weight factor is not a strong function of vehicle size.

5) The TPS weight factor for a common TPS design for all lunar return strategies and vehicles is approximately 6.5%.

6) The TPS weight calculated for the advanced blanket material CFBI was found to be 10% less than that for the FRCI-12/LI-900 insulation system.

7) The TPS weight for a 1.0-scale crew vehicle is 50% less than the original Apollo design as a result of flight experience and improved materials.

Acknowledgment

The authors would like to acknowledge the effort of R. M. Ondler, JSC, in developing the trajectories for the vehicles analyzed in this report.

References

[1]Lee, D. B., and Goodrich, W. D., "The Aerothermodynamic Environment of the Apollo Command Module During Superorbital Entry," NASA TND 6792, April 1972.

[2]Rochelle, W. C., and Rohan, R. A., "User's Manual for QRAD Entry Radiation Program," JSC-26059, Lockheed Engineering and Sciences Co., Rept. LESC-30452, Houston, TX, Nov. 1992.

[3]Ried, R. C., Jr., Rochelle, W. C., and Milhoan, J. D., "Radiative Heating to the Apollo Command Module: Engineering Prediction and Flight Measurement," NASA TM X-58091; April 1972.

[4]Williams, S. D., Gietzel, M. M., Rochelle, W. C., and Curry, D. M., "TPS Design for Aerobraking at Earth and Mars," NASA TM-104739, Aug. 1991.

[5]Murray, A. L., "Further Enhancements of the BLIMP Computer Code and User's Guide," Wright-Patterson Air Force Base, OH, Rept. AFWAL-TR-88-3010, June 30, 1988.

[6]Bartlett, E. P., Abbett, M. J., Nicolet, W. E., and Moyer, C. B., "Improved Heat-Shield Design Procedures for Manned Entry Systems, Part II—Application to Apollo," Aerotherm, Rept. 70-15, Part 2, June 1970.

[7]Lee, D. B., Bertin, J. J., and Goodrich, W. D., "Heat-Transfer Rate and Pressure Measurements Obtained During Apollo Orbital Entries," NASA TN D-6028, Oct. 1970.

[8]Williams, S. D., and Curry, D. M., "Thermal Protection Materials Thermophysical Property Data," NASA RP 1289, Dec. 1992.

[9]Chiu, S. A., and Pitts, W. C., "Reusable Surface Insulations for Reentry Spacecraft," AIAA Paper 91-0695, Jan. 1991.

[10]Williams, S. D., and Curry, D. M., "Prediction of Rigid Silica Based Insulation Conductivity," NASA TP 3276, Jan. 1993.

[11]Williams, S. D., "Revised User's Guide to the AESOP-STAB Computer Program—Cray Version," Lockheed Engineering and Sciences Co., Rept. LESC-29161, Houston, TX, Jan. 1991.

[12]Williams, S. D., "Users' Guide to the AESOP-THERM Computer Program—Cray Version," Lockheed Engineering and Sciences Co., Rept. LESC-28949, Houston, TX, Nov. 1990.

[13]Pavlosky, J. E., and St. Leger, L. G., "Apollo Experience Report—Thermal Protection System," NASA TND 7564, Jan. 1974.

R. K. Clark
Associate Editor